Fuzzy logic control based high step up converter for electric vehicle applications

Ravindranath Tagore Yadlapalli*

Department of Electrical and Electronics Engineering,
R.V.R. & J.C. College of Engineering,
Chowdavaram, Guntur, A.P – 522019, India
Email: yrtagore@gmail.com
*Corresponding author

Anuradha Kotapati

Department of Electrical and Electronics Engineering,
VNR Vignana Jyothi Institute of Engineering and Technology,
Bachupally, Hyderabad, T.S – 500090, India
Email: anuradha.saibabu@gmail.com

Srinivasa Rao Balusu

Department of Electrical and Electronics Engineering,
Velagapudi Ramakrishna Siddhartha Engineering College,
Vijayawada, A.P – 520007, India
Email: balususrinu@gmail.com

Abstract: At present, the electric vehicles (EVs) have a dominant role for visualising the pollution less environment. Moreover, it is important to design efficient power conditioning units for fulfilling the desired tasks. With advancements in the technology, the fuel cells (FCs) can provide a better solution for powering the EVs. However, their downside is the production of very low output voltage. Therefore, this necessitates a high step ratio DC-DC converter for providing the desired dc link voltage for DC-AC converter. This paper focuses on fuzzy logic control (FLC) based high gain DC-DC converter for EV applications. The fuzzy controllers are superior in dealing the nonlinearities and plant parameter variations without the need of strict mathematical modelling of the converter system. The converter is simulated with simple voltage mode control as well as FLC based voltage mode control. The MATLAB simulation results are compared for the above two control strategies with an emphasis on the steady state and dynamic regulations.

Keywords: fuel cells; electric vehicles; power converters; control strategies.

Reference to this paper should be made as follows: Yadlapalli, R.T., Kotapati, A. and Balusu, S.R. (2022) 'Fuzzy logic control based high step up converter for electric vehicle applications', *Int. J. Innovative Computing and Applications*, Vol. 13, No. 1, pp.41–56.

Biographical notes: Ravindranath Tagore Yadlapalli finished his under graduation in 2001 from the GITAM College of Engineering, Vishakhapatnam, AP and MTech from IITM in 2004. He completed his PhD from JNTU Hyderabad in 2018. He started his career as an Assistant Professor in the VRSEC, Vijayawada for one year. Later, he shifted to VEC, Vadlamudi. He is currently working as an Associate Professor in R.V.R. & J.C. CE.

Anuradha Kotapati finished her under graduation in 1992 from AU College of Engineering, Vishakhapatnam, Andhra Pradesh and MTech from Osmania University in 1997. She was her awarded PhD from Osmania University, Hyderabad in 2012. She started her career as an Assistant Professor at VNR VJIET, Hyderabad and continuing her services as a Professor and Dean Academics.

Srinivasa Rao Balusu finished his under graduation in 1994 from JNTU Kakinada and MTech from JNTU Anantapur in 1996. He was his warded PhD from JNTU Hyderabad in 2015. He has 23 years of teaching experience and is currently working as a Professor in Velagapudi Ramakrishna Siddhartha Engineering College.

1 Introduction

The step-up converters play an eminent role for boosting the voltage in case of fuel cell (FC) powered electric vehicle (EV) applications. Importantly, the EVs are replacing fossile fuel vehicles and thereby saving billions of dollars over the world (Das et al., 2017). The EVs have many advantages such as zero CO_2 emissions, low maintenance and high energy efficiency. The electric cars are more economical for transportation purposes. But, they are lacking of abundant number of charging stations. Furthermore, the flash charge batteries give flexibility in terms of six times faster charging and are more preferable compared to the lithium-ion batteries. They have the extraordinary features such as non-flammable, long life and non-toxic. Moreover, FC powered EVs are emerging all over the world (Ravindranath Tagore et al., 2019). The FCs present the following outstanding features.

- low emissions
- modularity
- scalability
- multi-fuel flexibility
- high reliability
- durability.

Each FC produces a very low voltage and therefore more efficient power conditioning units are required for boosting the FC stack voltage. Their performance depends on the internal effects such as ohmic, activation, mass transportation effects and also current ripples. Hence, efficient voltage regulators are required to grab better output voltage regulation, minimisation of current ripples and good dynamics. Hence, a lot of research is being carried out for developing high gain DC-DC converters along with good lifetime of the FCs. The FC stack voltage is fed to the dc link of DC-AC converter. The literature presents the advancements in the high step-up ratio converters (HSRCs) or high gain converters (Wu et al., 2015; Kardan et al., 2017; Zhang et al., 2018a, 2018b) with figures of merit such as high gain, voltage stresses of the power semiconductor devices, number of power components and finally overall cost of the converter system. Some converters are efficient in view of high conversion ratios. However, they are not favourable in terms of device stresses. This necessitates the devices with more voltage ratings and may not be acceptable in terms of overall cost of the system. Importantly, the number of devices can affect the efficiency as well as cost of the converter even though they exhibit better performance with better output voltage regulation, reduced current ripples and good converter dynamics. Therefore, it is important to obtain a compromise between the component number and converter gain in addition to the other desired features of the overall system.

This paper focuses on high gain R2P2 I-IIB BB+/ Bt+ converter (Zogogianni et al., 2019) which are derived from the family of reduced redundant power processing (R2P2) converters specifically for EV applications. This topology exhibits the features like good agglomeration of high step-up ratio as well as good efficiency and more suitable for high power applications. This topology has been implemented (Zogogianni et al., 2019) with simple voltage mode control (VMC) strategy. But, the design of VMC based converter topologies highly relies on the modelling techniques and their accuracy. The controller design may be worse due to the assumptions made while modelling the converters. It is also difficult to deal the nonlinearities such as temperature and saturation effects. On the other hand, fuzzy controllers do not need accurate mathematical modelling of the system and offers a linguistic approach to incorporate control algorithms in any power electronic converter systems. It is basically an adaptive and nonlinear control that can handle the plant parameter variations. Furthermore, another downside of VMC based DC-DC converter is the poor dynamics. This slow transient response can be improved with fuzzy logic control (FLC) based VMC. Many dc-dc converter topologies have been reported with FLC for EV applications (Leso et al., 2018; Omotoso et al., 2019; Metin et al., 2019; Amulya and Dhanalakshmi, 2019). A simple FLC based phase shifted PWM DC-DC converter is designed to control the output voltage (Leso et al., 2018). Importantly, the growth of EVs is hindered by the long charging intervals. Hence, a constant current FLC based DC-DC converter is designed without the need of tuning of a PI controller (Omotoso et al., 2019). The FLC has proved its effectiveness in minimising the charging time. A FLC based bidirectional DC-DC converter is designed in order to control the charging and discharging modes of a battery for EVs (Metin et al., 2019). The potential advantages of a FLC based resonant DC-DC converter is presented through extensive simulation studies (Amulya and Dhanalakshmi, 2019). Here, the performance of this converter is compared with the conventional PI controller based VMC. Due to the above attractive features, this paper presents the FLC based VMC instead of a PI based VMC for this high gain R2P2 I-IIB BB+/ Bt+ converter. This topology is able to provide a voltage gain of nearly nine (~9) for producing the desired output voltage of 400 V. On the other hand, the important aspects while designing the DC-DC converters are good load and line regulations over a wide range of operating conditions besides the good transient response. The simulation of FLC based VMC and PI based VMC is fulfilled with much more emphasis on load and line regulations. Different case studies are considered for analysing the performance of the high gain converter in terms of steady state voltage ripple, Transient Voltage Deviation (TVD) and Transient Settling Time (TST). This paper is organised as follows; Section 2 enlightens the fundamental aspects of HSRC and various control strategies in Section 3. Section 4 and Section 5 give the simulation results and conclusions.

2 DC-DC converter

Figure 1 depicts the wide voltage gain converter (Zogogianni et al., 2019). The HSRC input-output voltage relation is given by

$$\frac{V_O}{V_{in}} = \frac{1+D}{1-D} \tag{1}$$

where V_o and V_{in} are the output and input voltages, 'D' is the duty cycle of the HSRC.

Figure 1 Schematic of HSRC

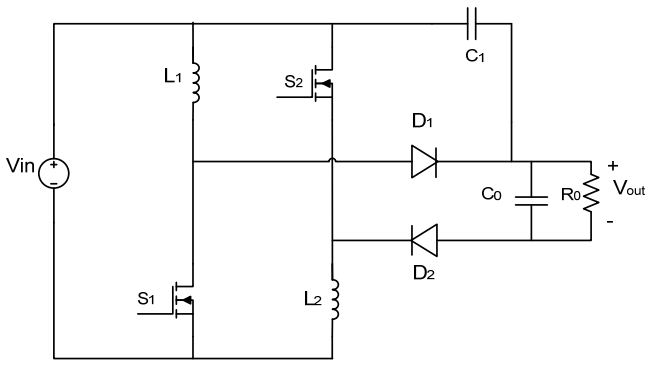

Source: Zogogianni et al. (2019)

3 Control strategies

3.1 Voltage mode controller

The dynamics of various dc-dc converters are interpreted with the aid of different modeling techniques which are reported in the literature (Karanet and Bunlaksananusorn, 2011; Yadlapalli and Kotapati, 2014). Out of them the attractive solution for modeling of converters is the state-space averaging. This approach features in grabbing of various control transfer functions based on equation (2). These transfer functions are useful for analysing the HSRC dynamics.

$$\begin{aligned} \frac{dx(\tilde{t})}{dt} &= A_s x(\tilde{t}) + B_s u(\tilde{t}) + B_i d(\tilde{t}) \\ y(\tilde{t}) &= C_s x(\tilde{t}) + E_s u(\tilde{t}) + E_i d(\tilde{t}) \end{aligned} \tag{2}$$

$$\begin{aligned} A_s &= A_{11}D + A_{22}(1-D) \\ B_s &= B_{11}D + B_{22}(1-D) \\ C_s &= C_{11}D + C_{22}(1-D) \\ E_s &= E_{11}D + E_{22}(1-D) \\ B_i &= (A_{11} - A_{22})X + (B_{11} - B_{22})U \\ E_i &= (C_{11} - C_{22})X + (E_{11} - E_{22})U \end{aligned}$$

where $u(\tilde{t})$ and $d(\tilde{t})$ are the small ac variations in the input vector and duty ratio. The vectors $x(\tilde{t})$ and $y(\tilde{t})$ are the corresponding small ac variations in the state and output vectors. $\frac{dx(\tilde{t})}{dt}$ is the derivate of the small signal variations. The matrices A_s, B_s, C_S, E_S, B_i, E_i are obtained based on the matrices A_{11}, A_{22}, B_{11}, B_{22}, C_{11}, C_{22}, E_{11}, E_{22}, and represent the network connections during on and off intervals of the MOSFET switch.

Equation (3) is obtained by applying Laplace transform to equation (2).

$$\begin{aligned} x(\tilde{s}) &= \begin{bmatrix} (SI-A)^{-1}B_s & (SI-A)^{-1}B_i \end{bmatrix} \begin{bmatrix} u(\tilde{s}) \\ d(\tilde{s}) \end{bmatrix} \\ y(\tilde{s}) &= \begin{bmatrix} C_s(SI-A)^{-1}B_s + E_s & C_s(SI-A)^{-1}B_i + E_i \end{bmatrix} \begin{bmatrix} u(\tilde{s}) \\ d(\tilde{s}) \end{bmatrix} \end{aligned} \tag{3}$$

Equation (3) gives the necessary small signal transfer functions. The transfer function required for VMC design is $\frac{\hat{v}_o(s)}{\hat{d}(s)}$. This transfer function plays a key role while designing the compensators in case of a VMC strategy.

3.2 Fuzzy logic controller

The effectiveness of a FLC highly (Yadlapalli et al., 2019; Yadlapalli and Kotapati, 2020; Castillo et al., 2016a, 2016b; Ontiveros-Robles et al., 2018; Sanchez et al., 2015) relies on the in depth technological view of the entire converter system. The FLC block diagram is shown in Figure 2. FLC features in simple operation and the control action depends on the setup of different well defined input conditions of the selected variables. The optimal performance of the converter system is realised using eminent Mamdani's implication approach combined with the defuzzification based on centre of area (COA) technique. In COA method (Bose, 1994; Cervantes and Castillo, 2015; Castillo, 2018), the crisp output Z_0 for the variable Z can be realised by taking the output fuzzy value $\mu_{out}(Z)$ area geometric centre, where $\mu_{out}(Z)$ is obtained by selecting the union of entire rules contributions with degree of freedom (DOF) greater than zero.

Figure 2 Block diagram of FLC based VMC

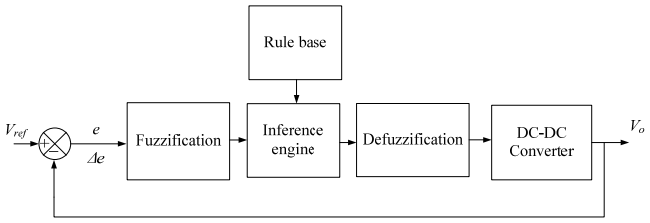

COA method is based on the general expression represented by

$$Z_0 = \frac{\int Z.\mu_{out}(Z)}{\int \mu_{out}(Z)dZ} \tag{4}$$

Using the discretised universe of discourse with the expression given as

$$Z_0 = \frac{\sum_{i=1}^{n} Z_i . \mu_{out}(Z_i)}{\sum_{i=1}^{n} \mu_{out}(Z_i)} \quad (5)$$

where Z_i represents the value of the discrete element, $\mu_{out}(Z_i)$ is the membership function (MF) value at the point Z_i, n is the number of discrete elements. FLC rule matrix is depicted in Table 1. The input scaling factor is realised with inputs ranging from –1 to +1. The attractive triangular shape MF arrangement infers that for any $e(k)$ input there is only one predominant fuzzy subset. The error e is given as

$$e(k) = V_{ref} - v_o(k) \quad (6)$$

where V_{ref} and $v_o(k)$ indicate the reference voltage and sampled load voltage at the k^{th} sampling instant.

$$ce(k) = e(k) - e(k-1) = v_o(k-1) - v_o(k) \quad (7)$$

where $e(k)$, $ce(k)$ and $e(k–1)$ represent the error, change in error at the kth sampling instant and the value of error at previous sampling time, $v_o(k–1)$ represent the load voltage at previous sampling time.

Table 1 Fuzzy logic control rule matrix

e / Δe	*Error*						
	NB	*NM*	*NS*	*ZE*	*PS*	*PM*	*PB*
NB	NB	NB	NB	NB	NM	NS	ZE
NM	NB	NB	NB	NM	NS	ZE	PS
NS	NB	NB	NM	NS	ZE	PS	PM
ZE	NB	NM	NS	ZE	PS	PM	PB
PS	NM	NS	ZE	PS	PM	PB	PB
PM	NS	ZE	PS	PM	PB	PB	PB
PB	ZE	PS	PM	PB	PB	PB	PB

The main objective of this paper is to realise attractive solution associated with the converter dynamics in terms of robustness against line voltage variations besides the load regulation. Another important aspect is regarding the dynamics of the FC. FCs are highly sensitive to current ripples and induces a negative effect on the converter system performance. Sometimes these effects are linked with the internal behaviour of the FC. Therefore, careful design is essential for achieving attractive performance. Moreover, the dynamics associated with FC should be perfectly matched while tuning the controllers as well as MFs. This is accomplished by trial and error approach using fuzzy logic toolbox in MATLAB software. For getting better dynamics in terms of TST even efficient methodologies namely ANFIS, neural network and genetic algorithms are chosen which will result in better tuning of the MFs for grabbing settling times of the order of µsec. Figure 3, Figure 4 and Figure 5 depict the MFs of different variables. In this paper, the converter is simulated with simple VMC as well as FLC based VMC. The MATLAB simulation results are presented for the above two control strategies with an emphasis on the steady state and dynamic regulations. The various figures of merit for the performance analysis are the steady state voltage ripple, TVD and TST.

Figure 3 Error MF (see online version for colours)

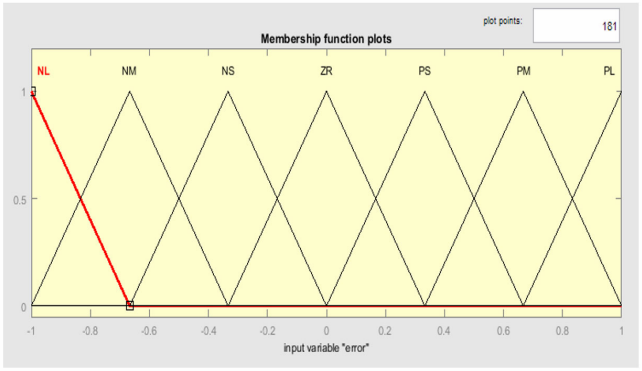

Figure 4 Changing error MF (see online version for colours)

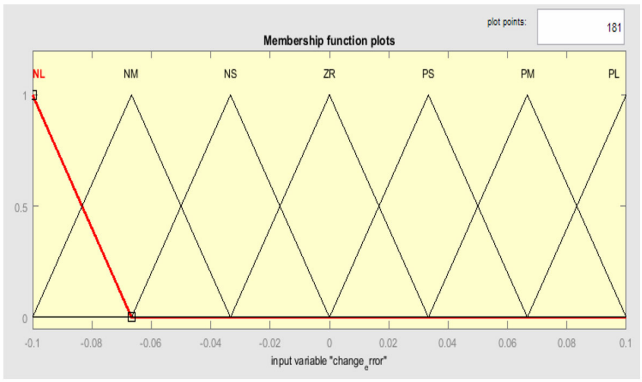

Figure 5 Output signal MF (see online version for colours)

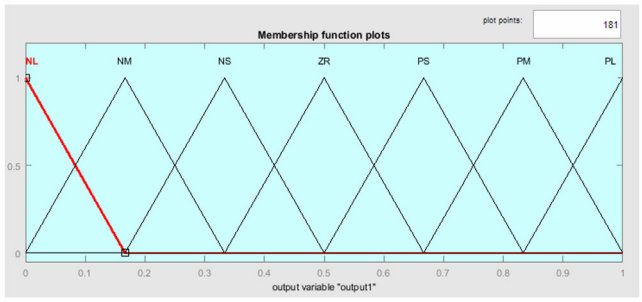

4 Simulation results

The performance of HSRC is analysed with the aid of distinct case studies. The specifications of HSRC are presented in Table 2. Figure 6 and Figure 7 show the MATLAB simulation diagrams of VMC as well as VMC based FLC for HSRC.

Figure 6 MATLAB Simulink circuit of HSRC with VMC (see online version for colours)

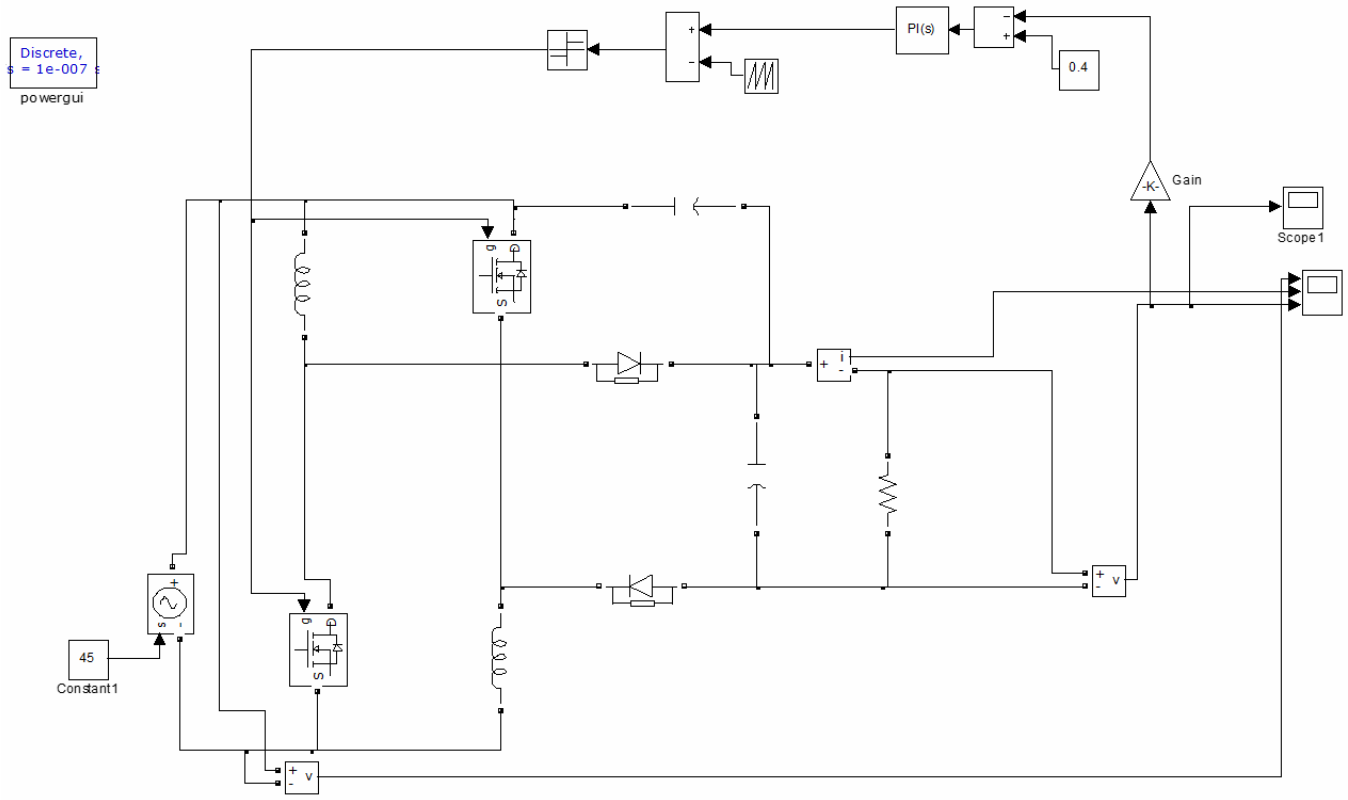

Figure 7 MATLAB Simulink circuit of HSRC with FLC based VMC (see online version for colours)

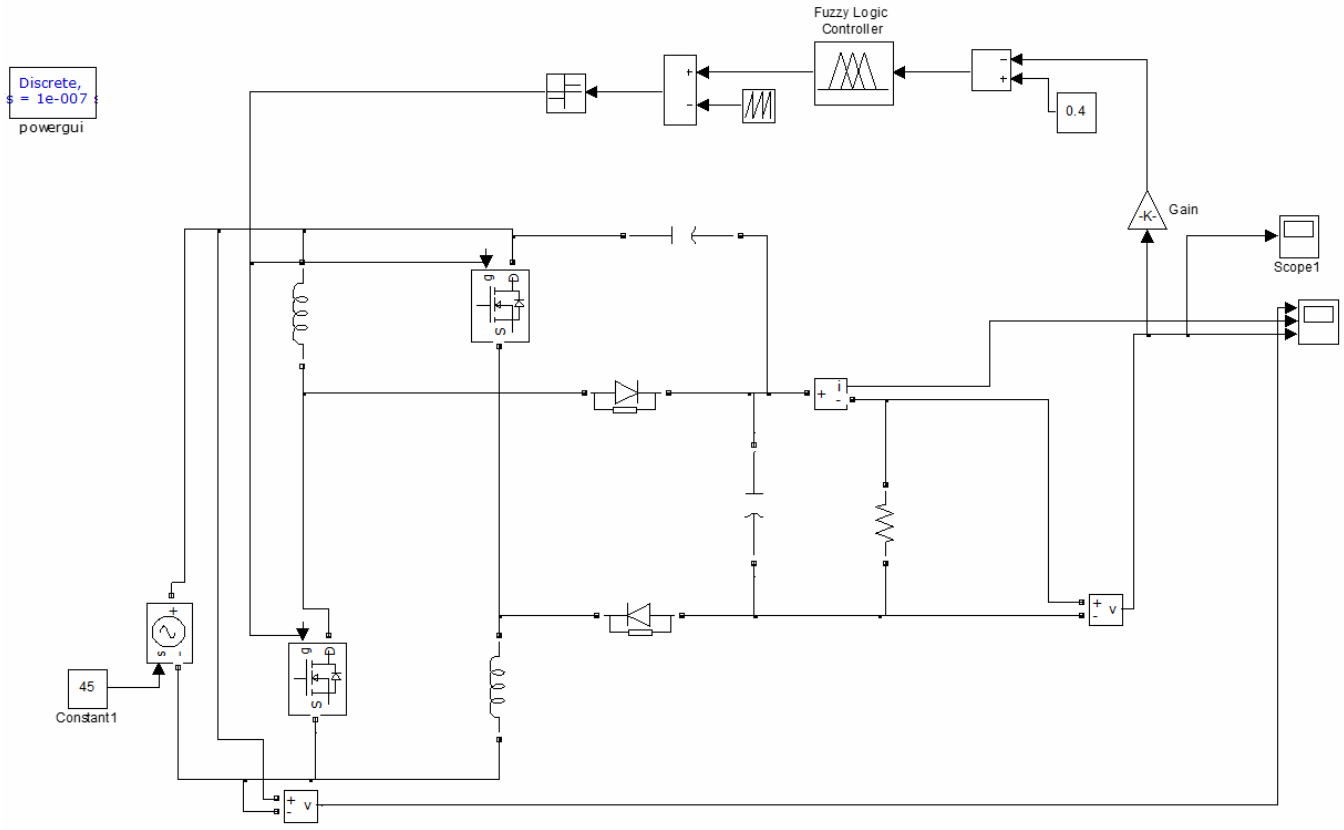

Table 2 Specifications of HSRC

Nominal parameter	*Value*
V_{in}	45 V
$L_1 = L_2$	300 µH
C_1	50 µF
C_o	280 µF
f_{sw}	50 kHz
V_0	400 V
Load $R_{min} – R_{max}$	80–160 Ω
K_P and K_I	100 & 0.2

4.1 Performance of VMC and VMC based FLC at 30V

VMC and FLC based VMC waveforms of HSRC are shown in Figure 8(a) and Figure 9(a). At constant load current of 5A, the steady state voltage ripple with VMC is ±1.5%, whereas it is ±1.05% in case of FLC based VMC, which are observed in the magnified waveforms of Figure 8(b) and Figure 9(b).

Figure 8 (a) HSRC waveforms with VMC at V_{in} = 30V and constant load current (I_o) of 5A (b) Output voltage ripple with VMC at V_{in} = 30V & I_o = 5A

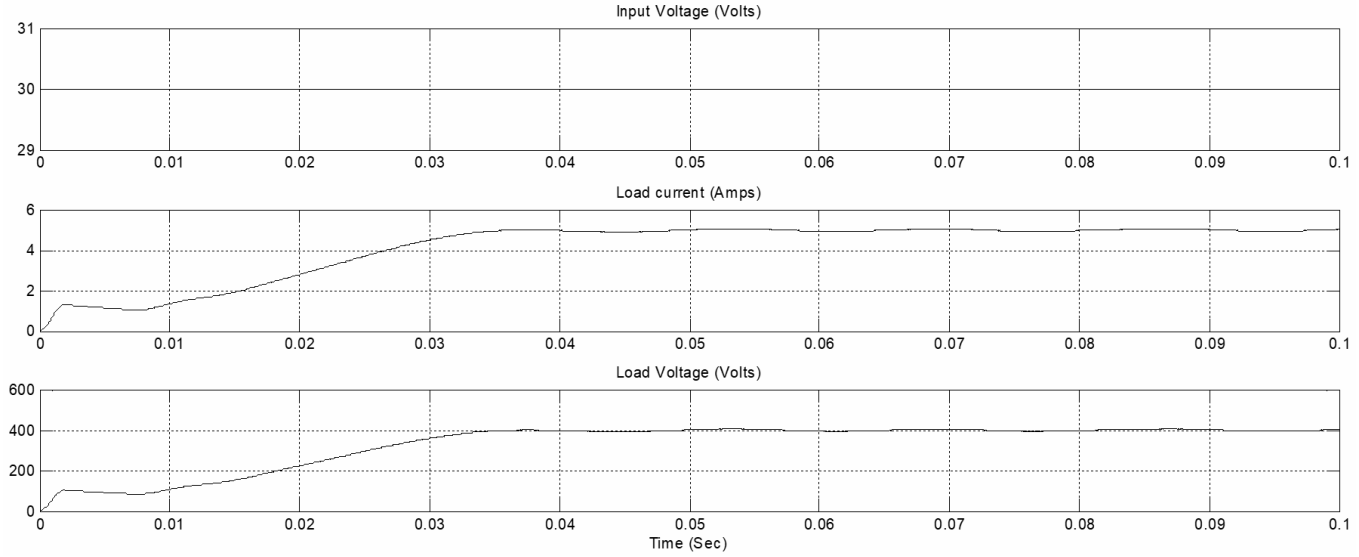

(a)

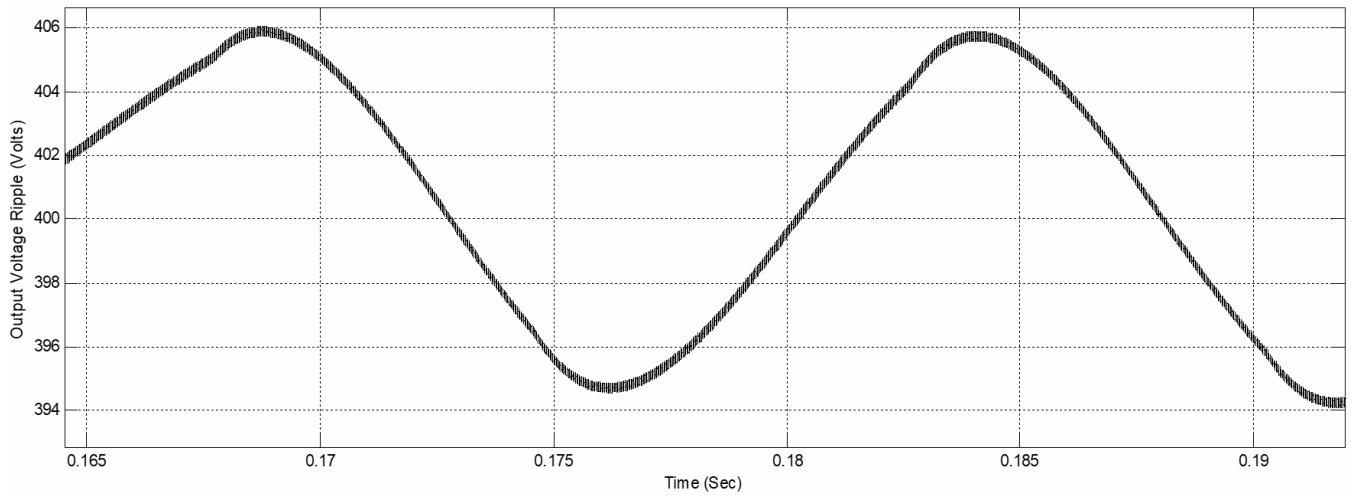

(b)

Figure 9 (a) HSRC waveforms with FLC based VMC at V_{in} = 30V & I_o = 5A (b) Output voltage ripple with FLC based VMC at V_{in} = 30V & I_o = 5A

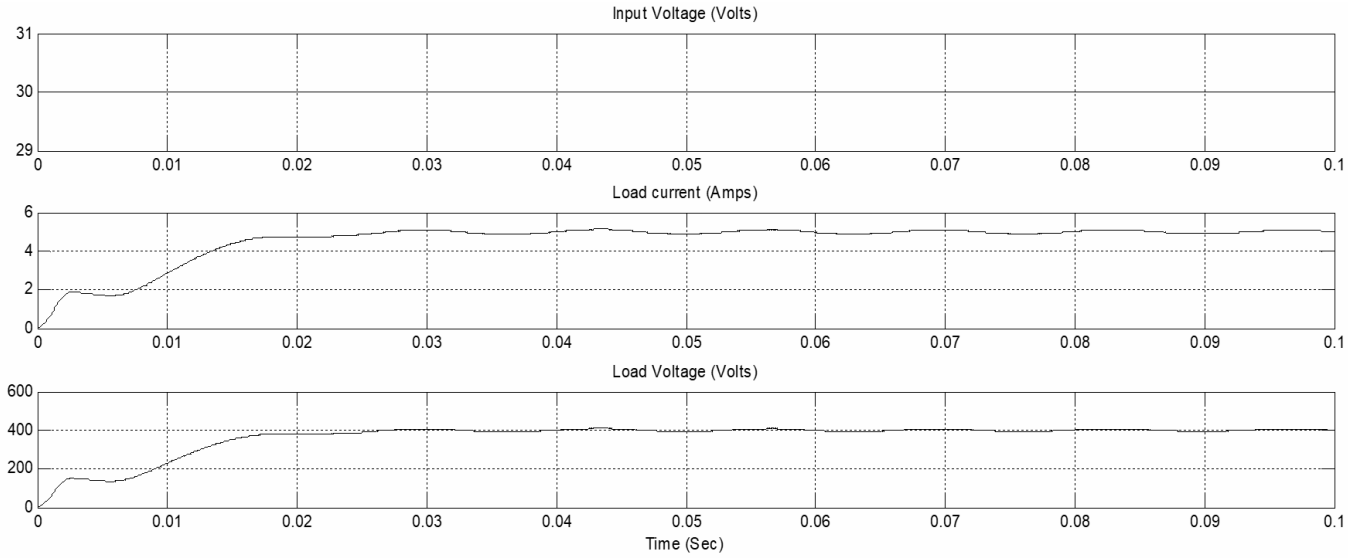

(a)

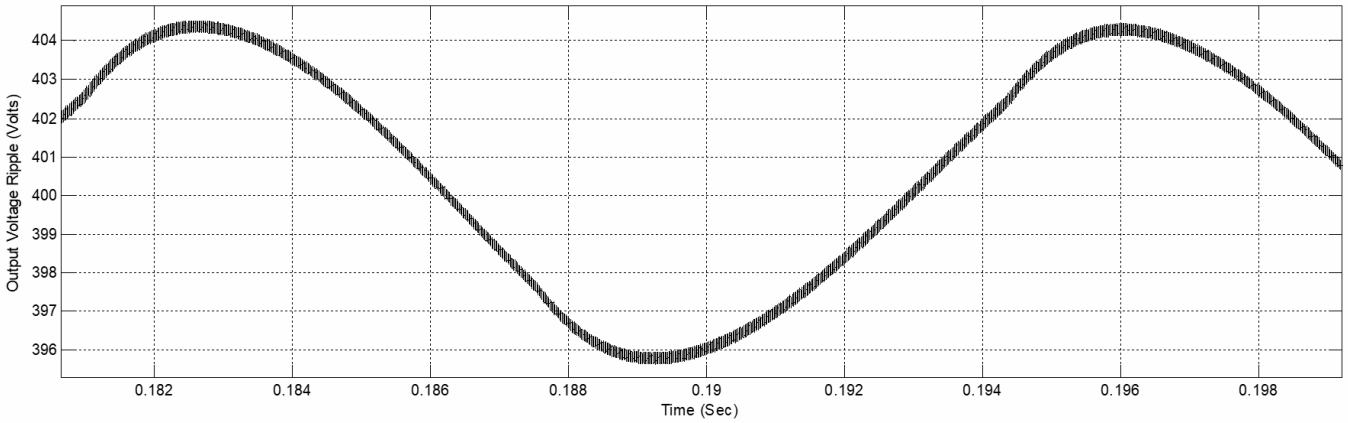

(b)

Figure 10 (a) HSRC waveforms with VMC at V_{in} = 45V & I_o = 5A (b) Output voltage ripple with VMC at V_{in} = 45V & I_o = 5A

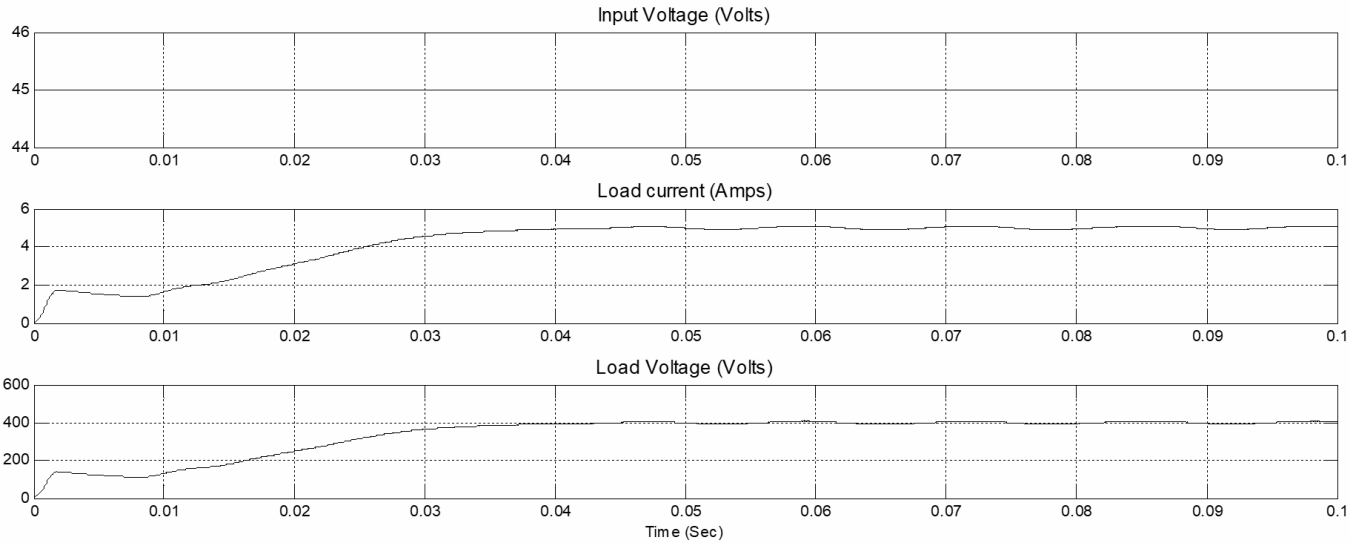

(a)

Figure 10 (a) HSRC waveforms with VMC at V_{in} = 45V & I_o = 5A (b) Output voltage ripple with VMC at V_{in} = 45V & I_o = 5A (continued)

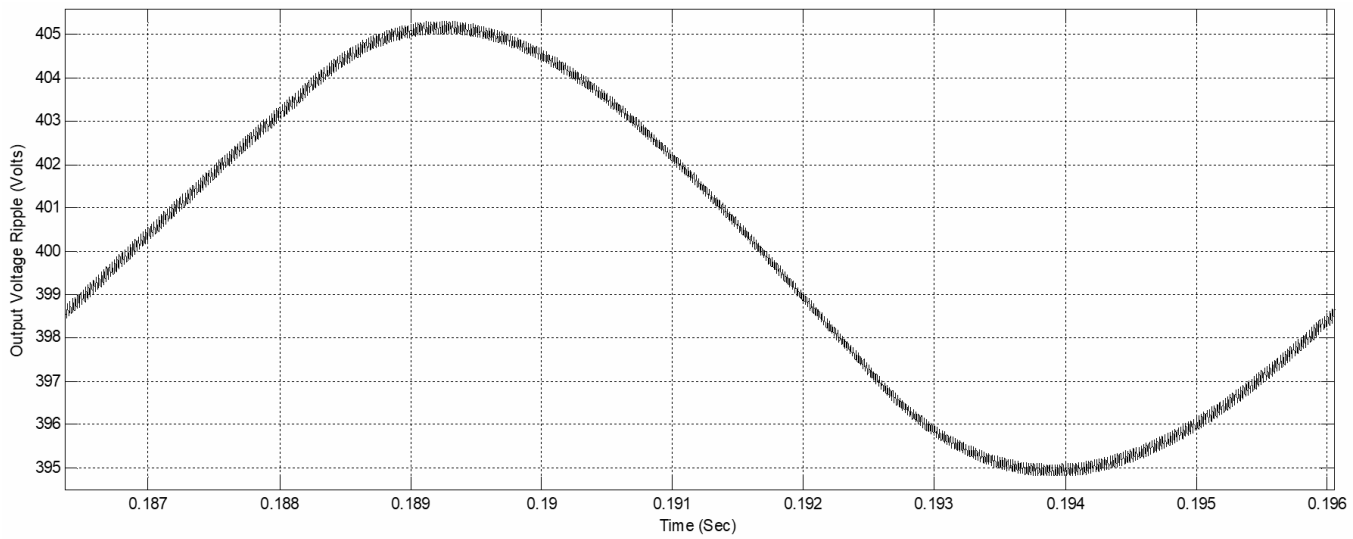

(b)

Figure 11 (a) HSRC waveforms with FLC based VMC at V_{in} = 45V & I_o = 5A (b) Output voltage ripple with FLC based VMC at V_{in} = 45V & I_o = 5A

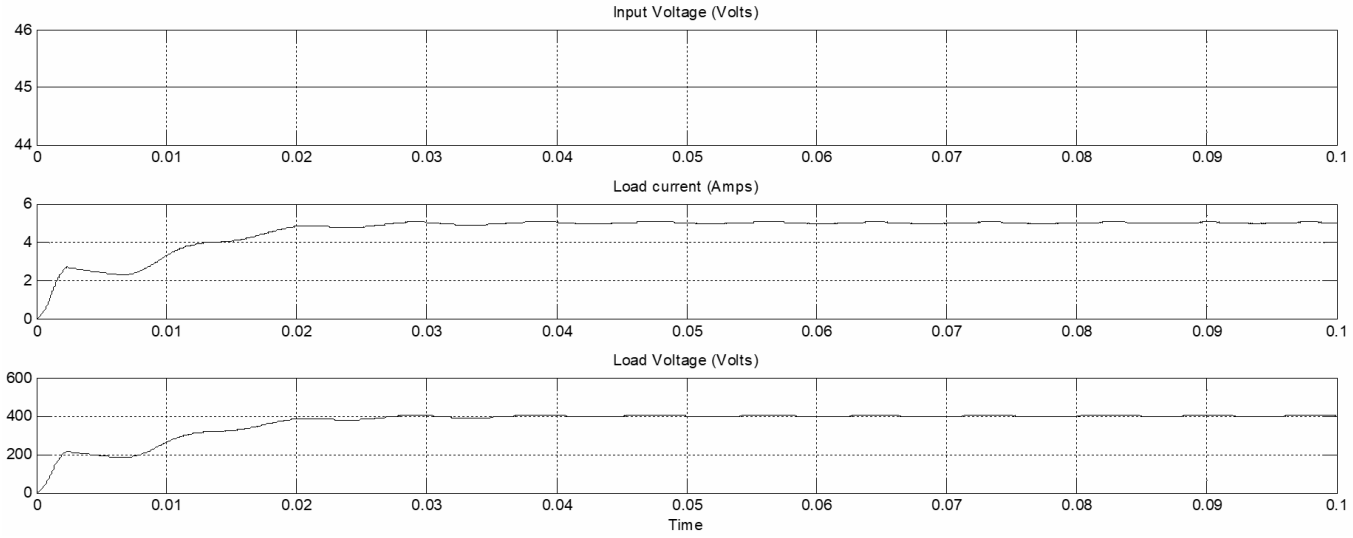

(a)

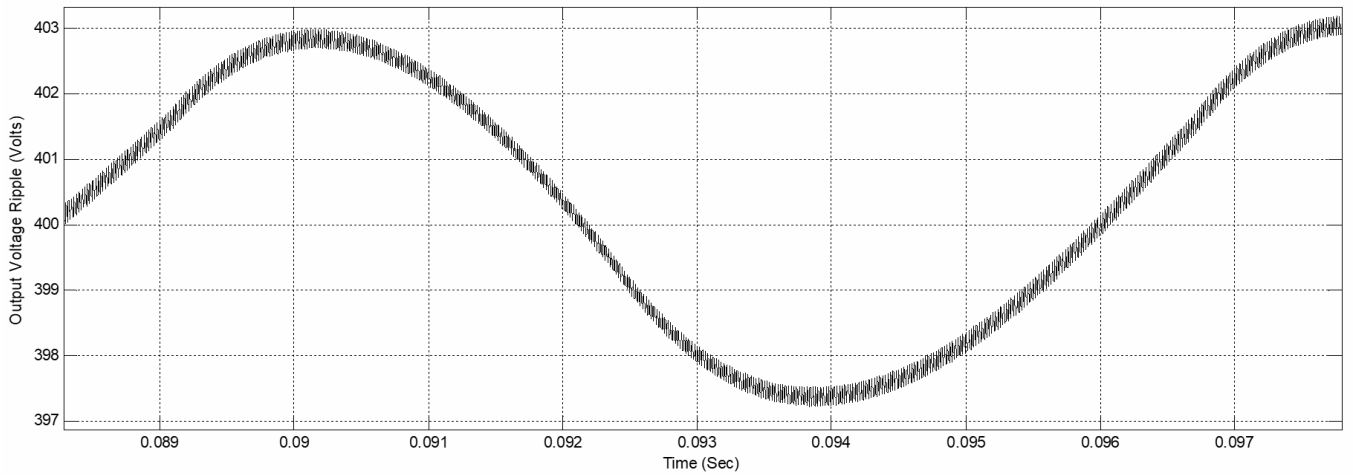

(b)

Figure 12 (a) HSRC waveforms with VMC at V_{in} = 120V & I_o = 5A (b) Output voltage ripple with VMC at V_{in} = 120V & I_o = 5A

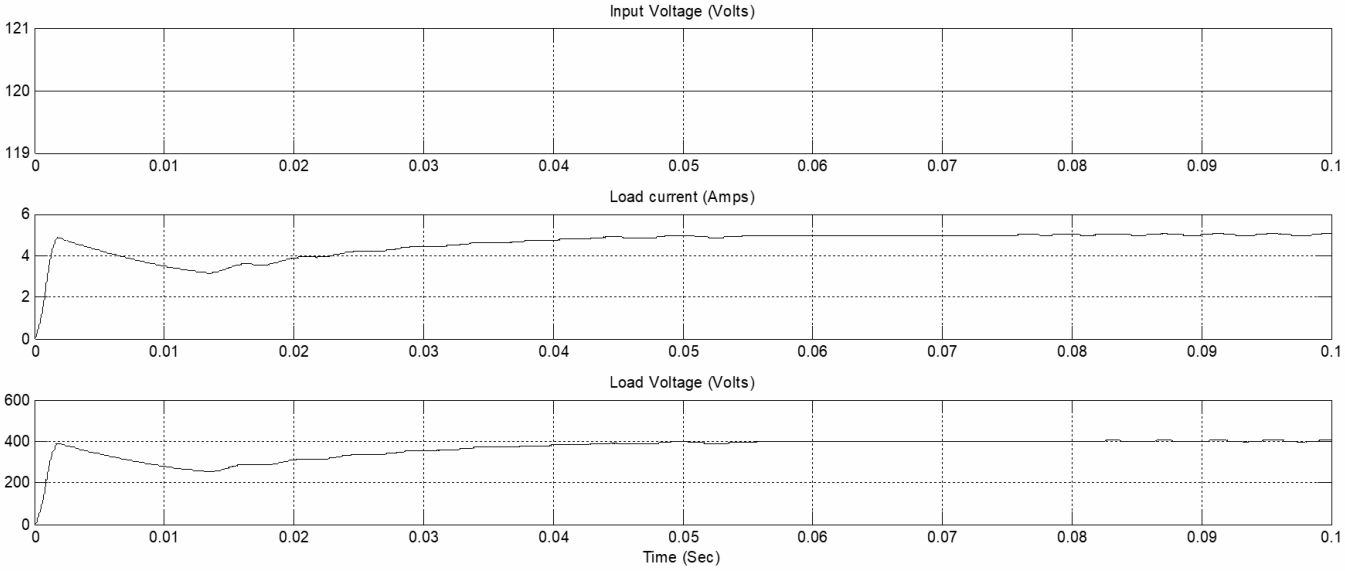

(a)

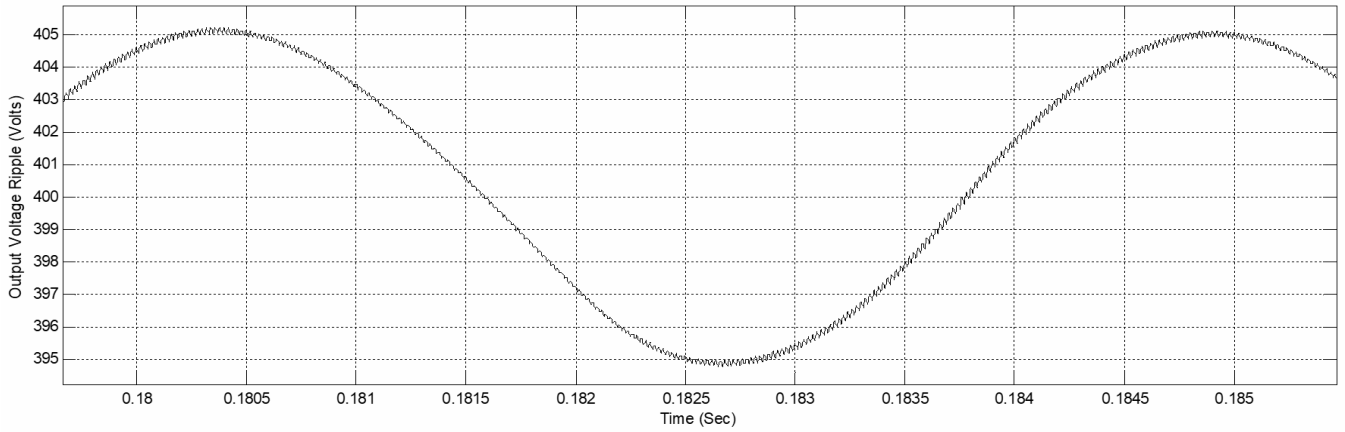

(b)

Figure 13 (a) HSRC waveforms with FLC based VMC at V_{in} = 120V & I_o = 5A (b) Output voltage ripple with FLC based VMC at V_{in} = 120V & I_o = 5A

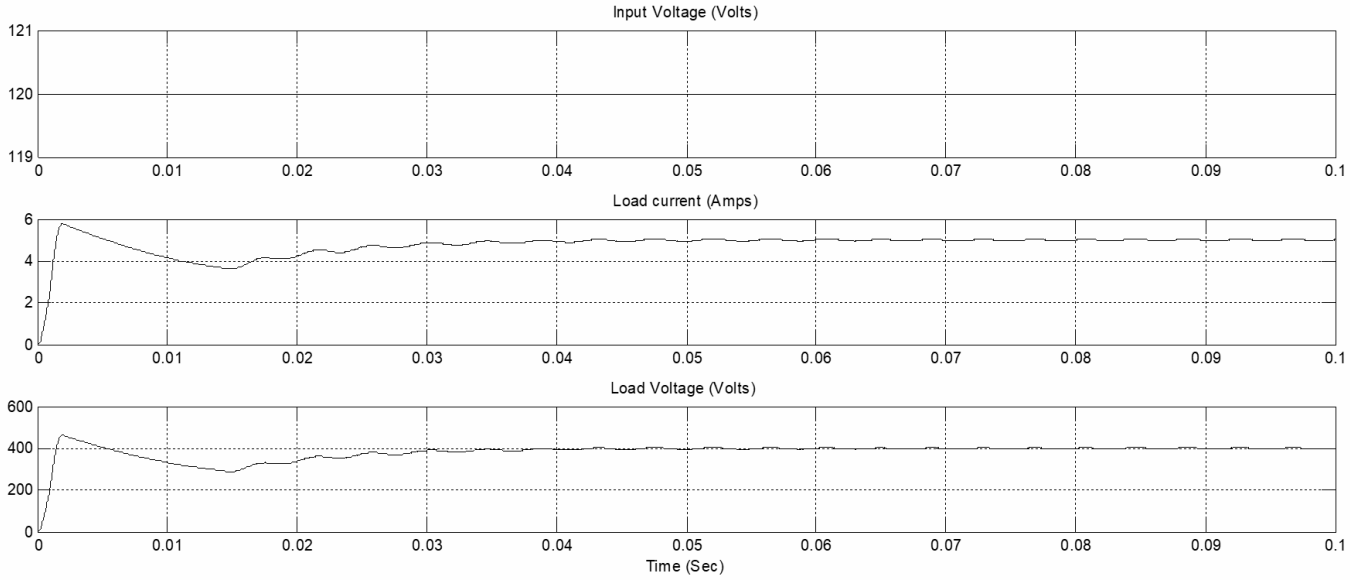

(a)

Figure 13 (a) HSRC waveforms with FLC based VMC at V_{in} = 120V & I_o = 5A (b) Output voltage ripple with FLC based VMC at V_{in} = 120V & I_o = 5A (continued)

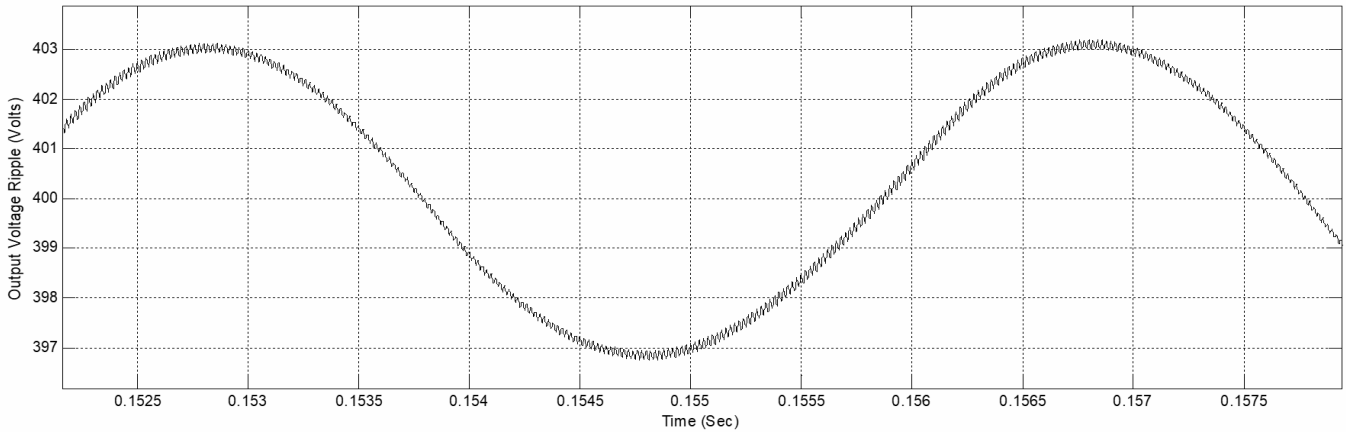

(b)

Figure 14 (a) HSRC waveforms with VMC at V_{in} = 30V & step load current (I_o) of 2.5A – 5A (b) Magnified HSRC waveforms with VMC at V_{in} = 30V & step I_o of 2.5A – 5A

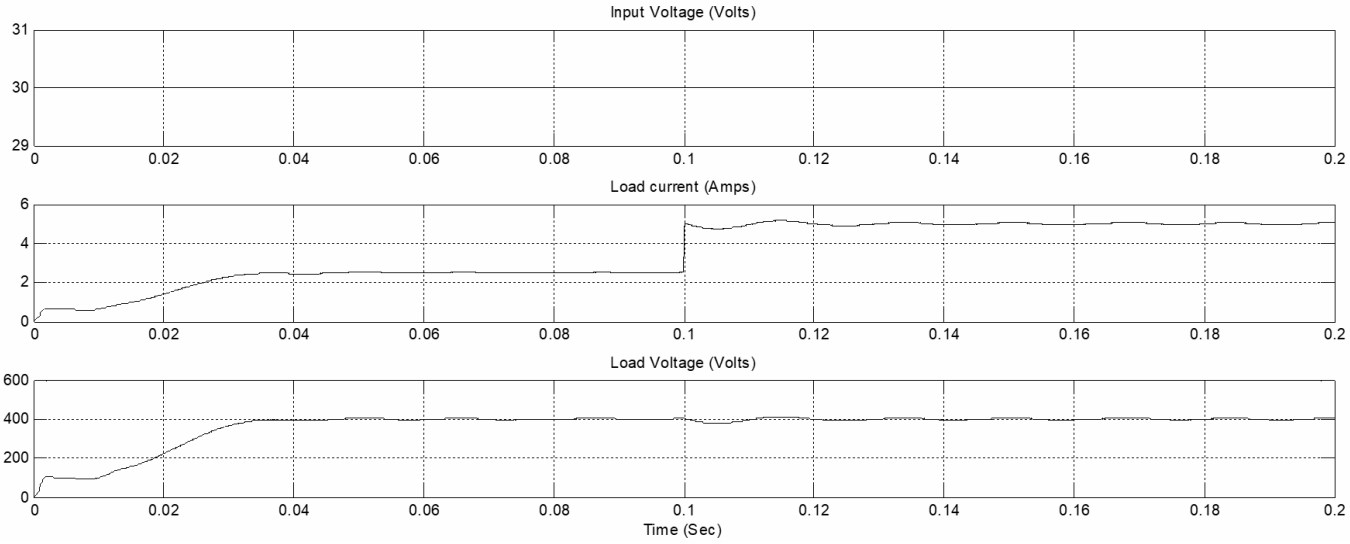

(a)

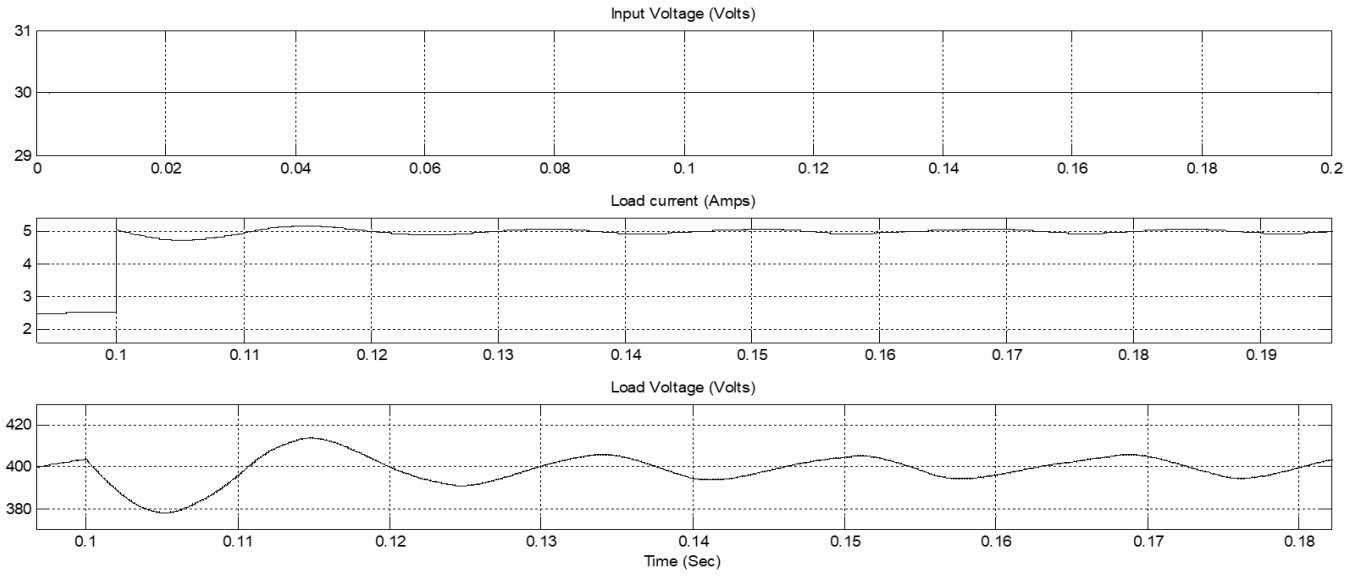

(b)

Figure 15 (a) HSRC waveforms with FLC based VMC at V_{in} = 30V & step I_o of 2.5A – 5A (b) Magnified HSRC waveforms with FLC based VMC at V_{in} = 30V & step I_o of 2.5A – 5A

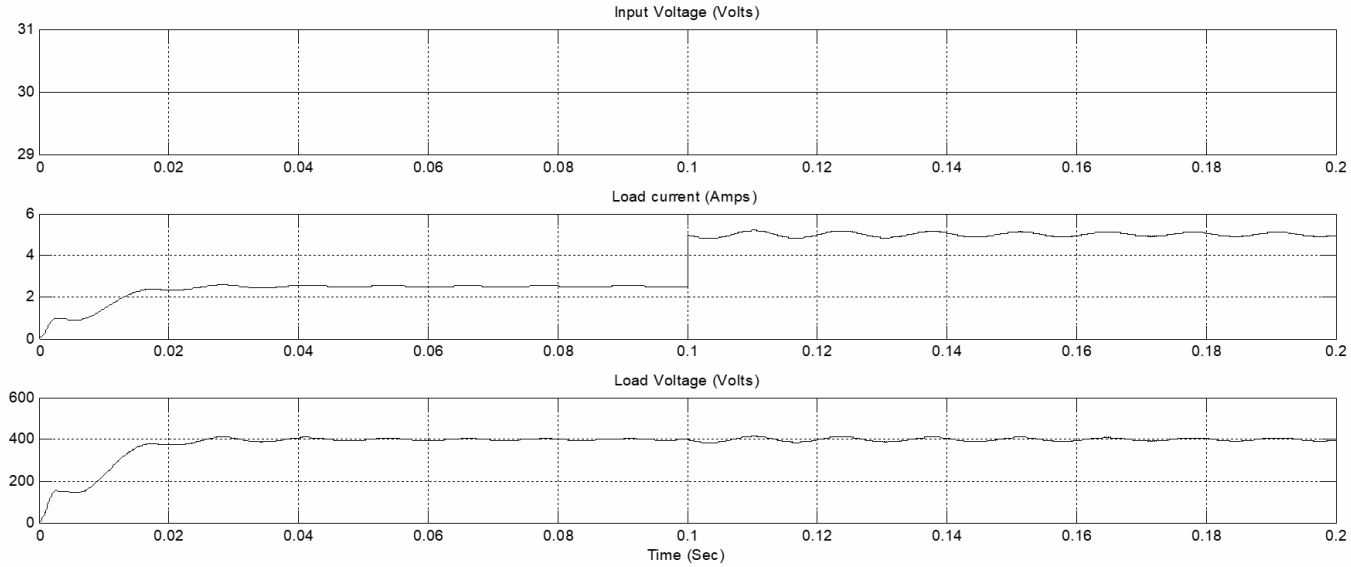

(a)

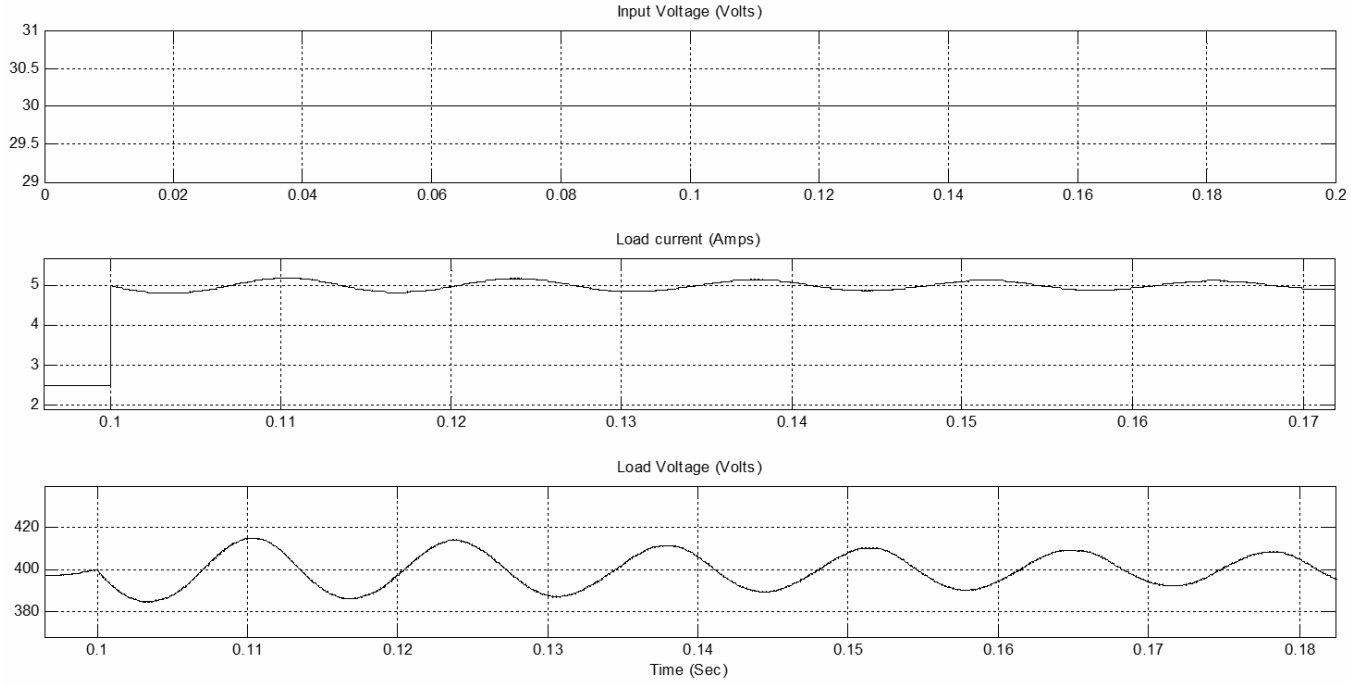

(b)

4.2 Performance of VMC and VMC based FLC at 45V

VMC and FLC based VMC waveforms of HSRC are shown in Figure 10(a) and Figure 11(a). At constant load current of 5A, the steady state voltage ripple is ±1.25% with VMC, whereas it is ±0.75% in case of FLC based VMC, which are observed in the magnified waveforms of Figure 10(b) and Figure 11(b).

4.3 Performance of VMC and VMC based FLC at 120V

VMC and FLC based VMC waveforms of HSRC are shown in Figure 12(a) and Figure 13(a). At constant load current of 5A, the steady state voltage ripple is ±1.25% with VMC, whereas it is ±0.8% in case of FLC based VMC, which are observed in the magnified waveforms of Figure 12(b) and Figure 13(b).

Figure 16 (a) HSRC waveforms with VMC at V_{in} = 45V & step I_o of 2.5A – 5A (b) Magnified HSRC waveforms with VMC at V_{in} = 45V & step I_o of 2.5A – 5A

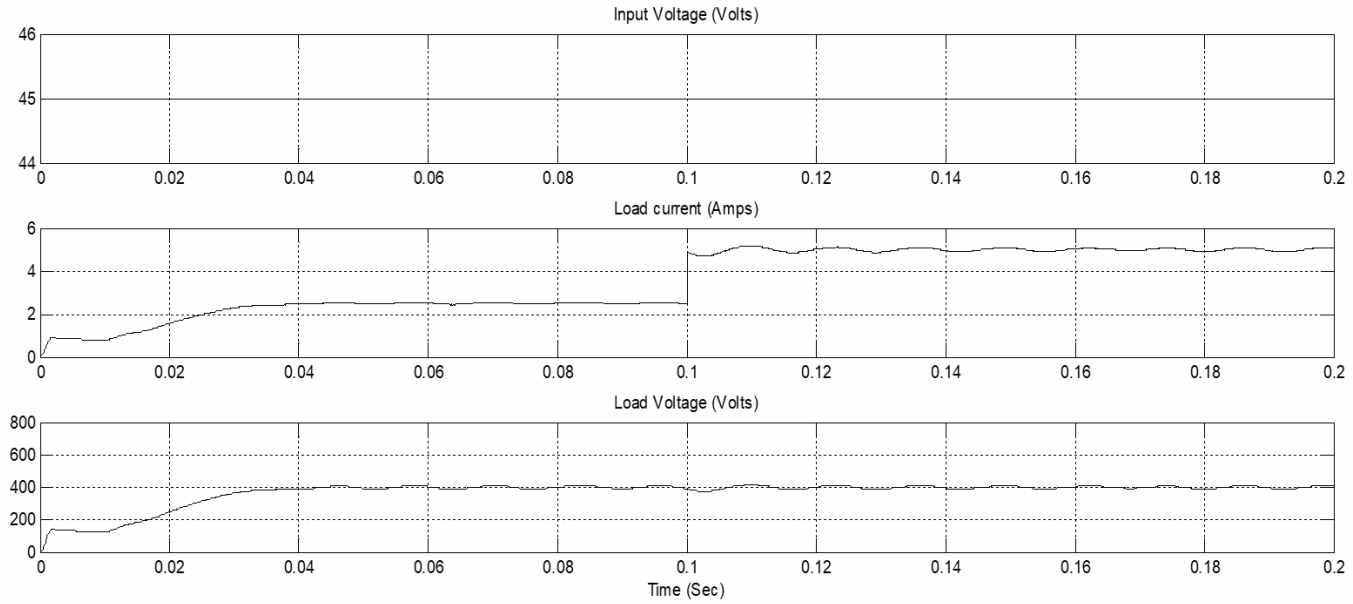

(a)

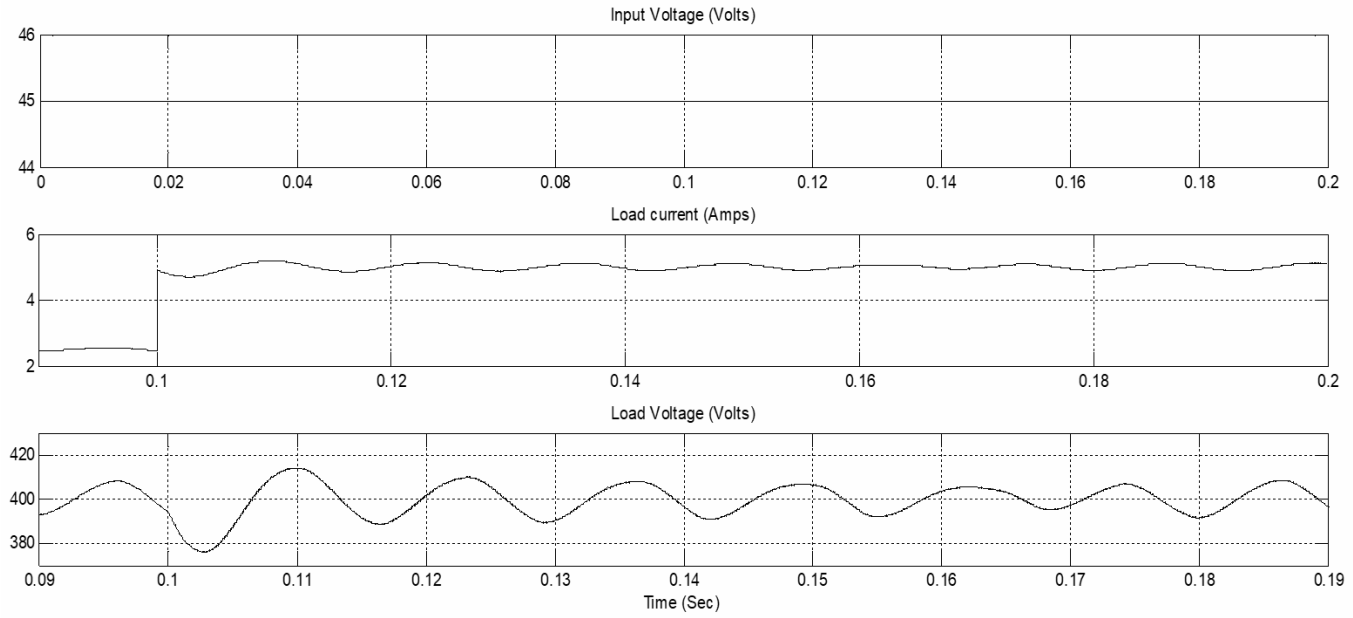

(b)

4.4 Performance of VMC and VMC based FLC for load transition at 30V

Figures 14(a) and 14(b) present the VMC based HSRC wherein the TVD during step-up load transition (2.5A to 5A) is –22V (–5.5%) with a TST of 0.08sec. Whereas in case of FLC based VMC, these values are at –16V (–4%) and 0.045 sec as shown in Figures 15(a) and 15(b).

4.5 Performance of VMC and VMC based FLC for load transition at 45V

Figures 16(a) and 16(b) present the VMC based HSRC wherein the TVD during step-up load transition (2.5A to 5A) is –24V (–6%) with a TST of 0.06sec. Whereas in case of FLC based VMC, these values are at –13V (–3.25%) and 0.0225 sec as shown in Figures 17(a) and 17(b).

Figure 17 (a) HSRC waveforms with FLC based VMC at V_{in} = 45V & step I_o of 2.5A – 5A (b) Magnified HSRC waveforms with FLC based VMC at V_{in} = 45V & step I_o of 2.5A – 5A

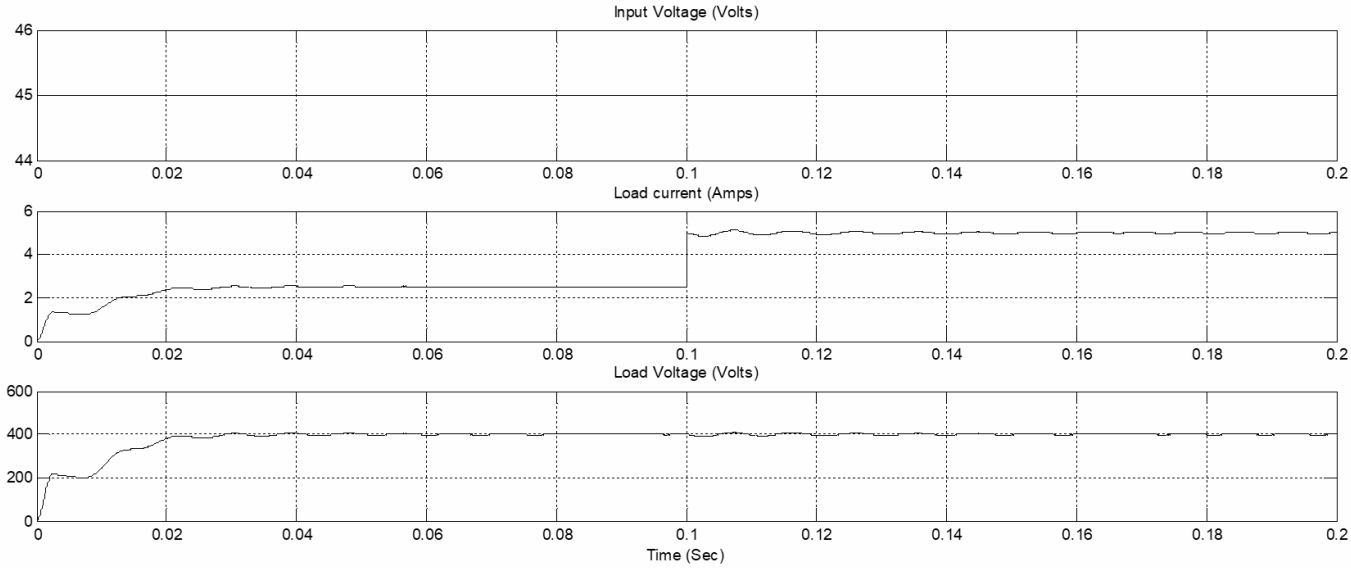

(a)

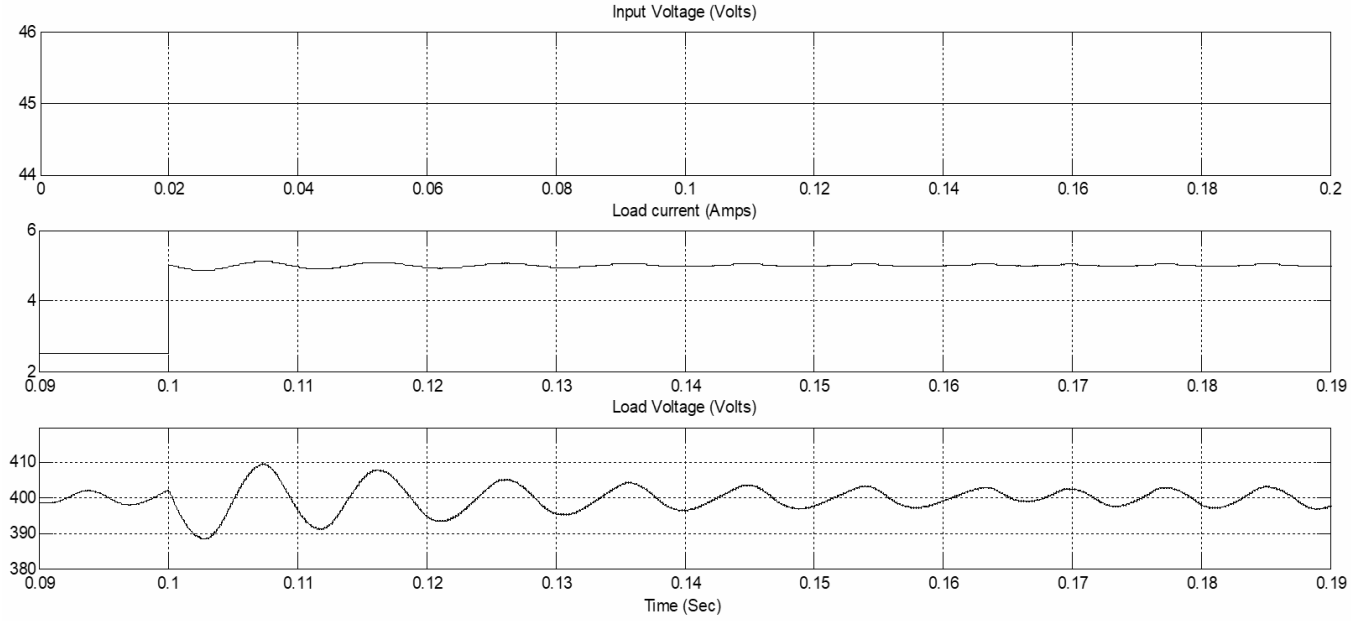

(b)

4.6 Performance of VMC and VMC based FLC for 45V – 30V step input voltage

Figures 18(a) and 18(b) present the VMC and FLC based VMC for a step input voltage from 45V – 30V. The FLC based VMC exhibits excellent performance with a TST of 0.025 sec as compared to 0.08sec in case of VMC. Moreover, the output waveforms are free from oscillations or peaks.

4.7 Performance of VMC and VMC based FLC for 45V – 120V step input voltage

Figures 19(a) and 19(b) present the VMC and FLC based VMC for a step input voltage from 45V – 120V. The FLC based VMC exhibits good performance with a TST of 0.045 sec as compared to 0.08sec in case of VMC. However, some peaks are observed in the output voltage and current waveforms due to a wide variation in the input voltage.

Figure 18 (a) HSRC waveforms with VMC at 45V – 30V step input voltage (V_{in}) (b) HSRC waveforms with FLC based VMC at 45V – 30V step V_{in}

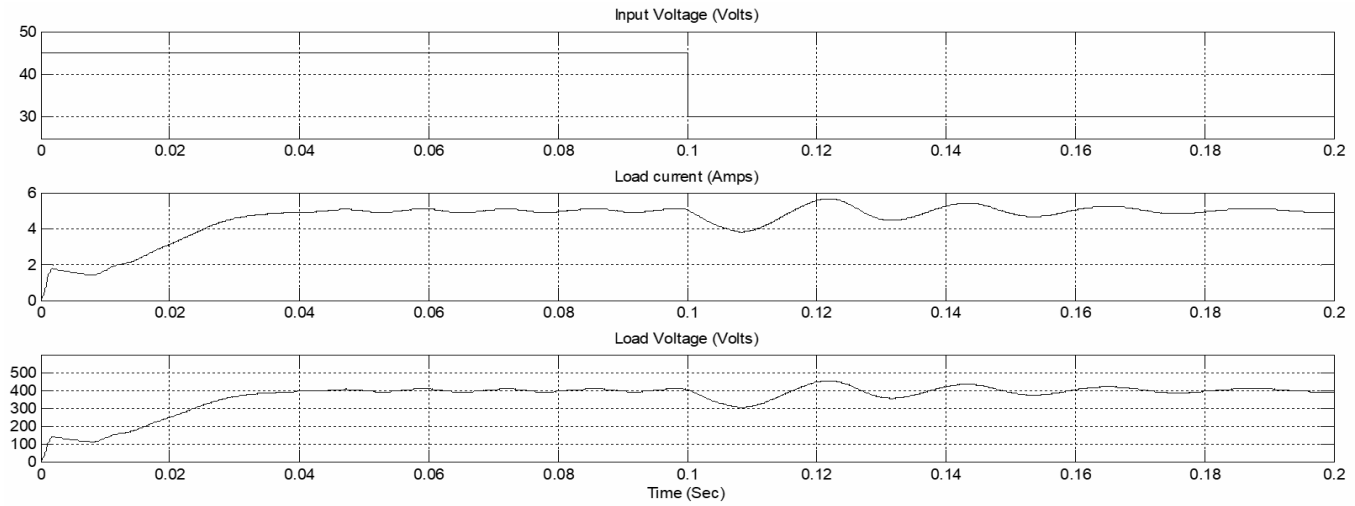

(a)

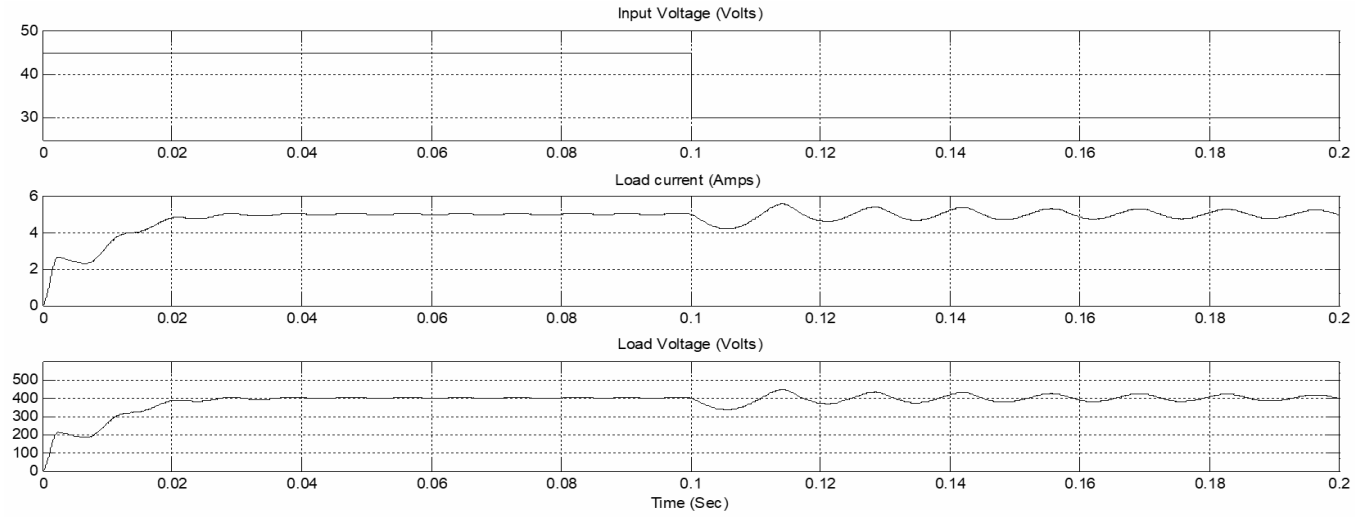

(b)

Figure 19 (a) HSRC waveforms with VMC at 45V-120V step V_{in} (b) HSRC waveforms with FLC based VMC at 45V-120V step V_{in}

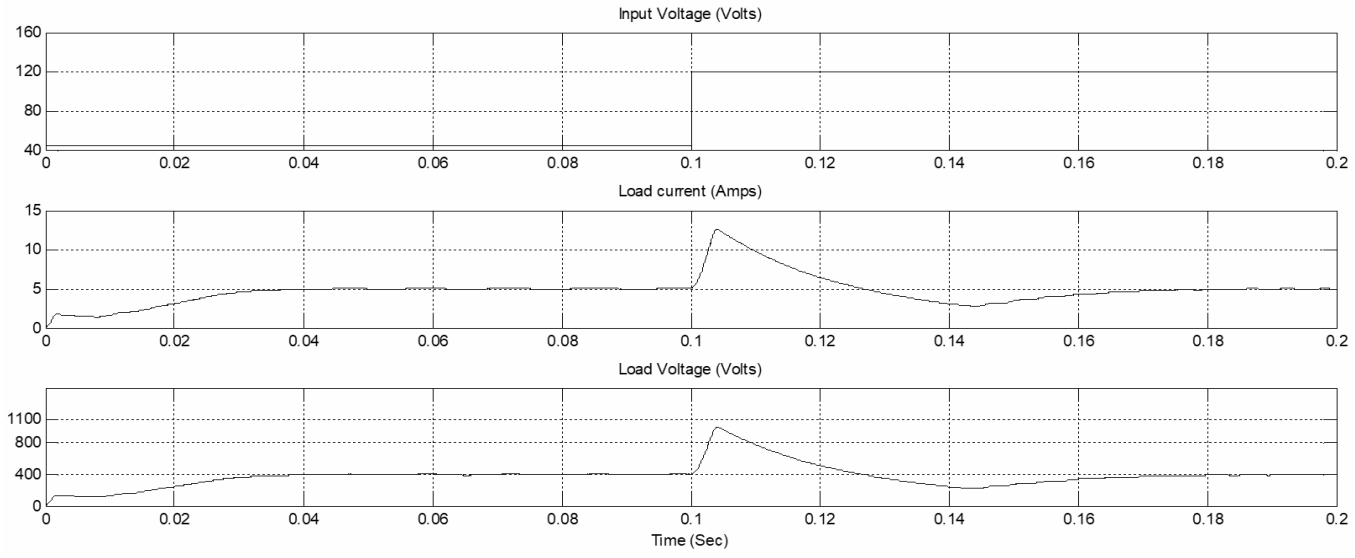

(a)

Figure 19 (a) HSRC waveforms with VMC at 45V-120V step V_{in} (b) HSRC waveforms with FLC based VMC at 45V-120V step V_{in} (see online version for colours)

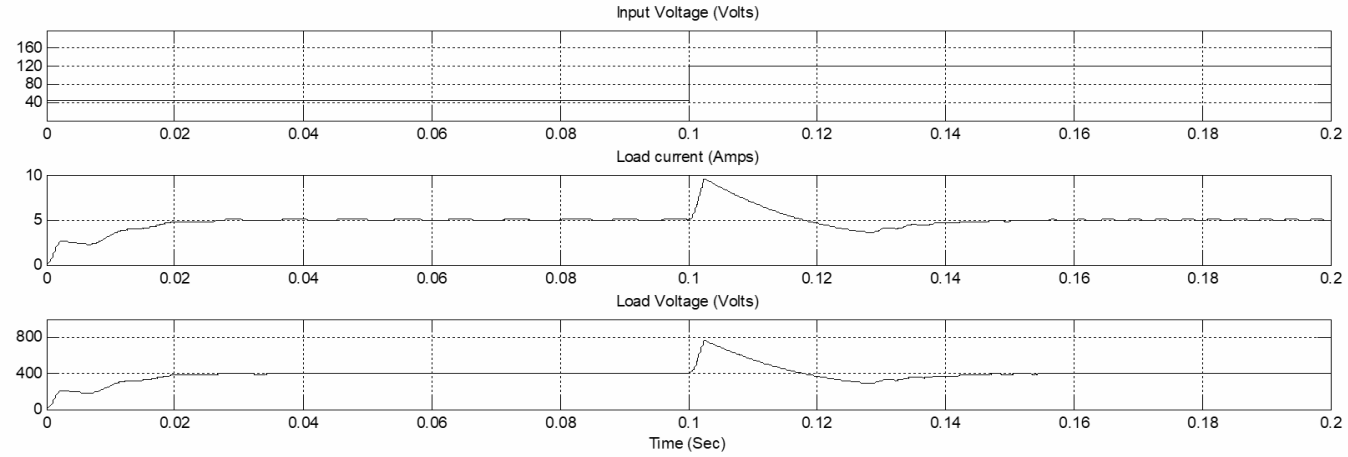

(b)

Table 3 HSRC performance in steady state

Input voltage	*HSRC with VMC*		*HSRC with FUZZY based VMC*	
	Steady state voltage deviation	$\frac{\Delta v_0}{\text{Desied output voltage}} \times 100\%$	*Steady state voltage deviation*	$\frac{\Delta v_0}{\text{Desied output voltage}} \times 100\%$
30 V	± 6 V	± 1.5%	± 4.2 V	± 1.05%
45 V	± 5 V	±1.25%	± 3 V	± 0.75%
120 V	± 5 V	± 1.25%	± 3.2 V	± 0.8%

Table 4 HSRC performance in transient conditions

Input voltage	*HSRC with VMC*		*HSRC with FUZZY based VMC*	
	TVD Step-up load transient	*TST (sec)*	*TVD Step-up load transient*	*TST (sec)*
30 V	–22 V (–5.5 %)	0.08	– 16 V (–4 %)	0.045
45 V	–24 V (–6 %)	0.06	–13 V (–3.25 %)	0.0225
120 V	–8 V (–2%)	0.003	–5.5 V (–1.375%)	0.001

4.8 Outcomes with VMC and FLC based VMC for HSRC

The performance of HSRC is shown in Table 3 with simple VMC as well as FLC based VMC at different input voltage conditions of 30V, 45V and 120V, the load is kept constant at 5A. The steady state voltage deviation and settling times are found to be good with FLC based VMC as compared to simple VMC. Table 4 shows the different case studies at 30V, 45V and 120V for evaluating the transient performance. The critical issues under consideration are the TVD and TST of the output voltage. During a sudden load disturbance, the output voltage settles in few msec in case of FLC based VMC as compared to simple VMC. On the other hand, the simulation results related with input voltage variations are seen well with FLC based VMC. The different case studies shown in Table 3 and Table 4 highlight the fact that the FLC based VMC is predominantly good in transient as well as steady state operating conditions as compared to simple VMC.

5 Conclusions

This paper highlights the performance features of a high step-up DC-DC converter specifically designed for EV applications. The simulation study is focused on steady state as well as dynamic regulations of the HSRC. The various figures of merit for the performance analysis are namely steady state voltage ripple, TVD and TST. FLC based VMC has exhibited good performance in view of the above significant aspects as compared to the VMC strategy. From the simulation results it is apparent that this converter is well suited as a power conditioning unit for FC powered EVs. Moreover, this research work can be further extended for high power applications along with the realisation of a fuzzy based current mode controller.

References

Amulya, N. and Dhanalakshmi, R. (2019) 'Analysis of fuzzy logic control based resonant DC-DC converter for high voltage gain', *2019 International Conference on Intelligent Computing and Control Systems (ICCS)*, Madurai, India, pp.1074–1079.

Bose, B.K. (1994) 'Expert system, fuzzy logic and neural network applications in power electronics and motion control', *Proc. IEEE*, Vol. 82, No. 8, pp.1303–1323.

Castillo, O. (2018) 'Towards finding the optimal n in designing type-n fuzzy systems for particular classes of problems: a review', *Appl. Comput. Math.*, Vol. 17, No. 1, pp.3–9.

Castillo, O., Amador-Angulo, L., Castro, J.R. and Garcia-Valdez, M. (2016a) 'A comparative study of type-1 fuzzy logic systems, interval type-2 fuzzy logic systems and generalized type-2 fuzzy logic systems in control problems', *Inf. Sci.*, Vol. 354, pp.257–274.

Castillo, O., Cervantes, L., Soria, J., Sanchez, M. and Castro, J.R. (2016b) 'A generalized type-2 fuzzy granular approach with applications to aerospace', *Information Sciences*, Vol. 354, pp.165–177.

Cervantes, L. and Castillo, O. (2015) 'Type-2 fuzzy logic aggregation of multiple fuzzy controllers for airplane flight control', *Information Sciences*, Vol. 324, pp.247–256.

Das, H.S., Tan, C.W. and Yatim, A.H.M. (2017) 'Fuel cell hybrid electric vehicles: a review on power conditioning units and topologies', *Renewable and Sustainable Energy Reviews*, Vol. 76, No. 1, pp.268–291.

Karanet, K. and Bunlaksananusorn, C. (2011) 'Modelling of a quadratic buck converter', *Proc. Int. Conf. Eighth Electrical Engineering Electronics, Computer, Telecommunications and Information Technology*, pp.764–767.

Kardan, F., Alizadeh, R. and Banaei, M.R. (2017) 'A new three input DC/DC converter for hybrid PV/FC/battery applications', *IEEE Trans. Power Electron.*, Vol. 5, No. 4, pp.1771–1778.

Leso, M., Zilkova, J. and Girovsky, P. (2018) 'Development of a simple fuzzy logic controller for DC-DC converter', *2018 IEEE 18th International Power Electronics and Motion Control Conference (PEMC)*, Budapest, pp.86–93.

Metin, N.A., Boyar, A. and Kabalci, E. (2019) 'Design and analysis of bi-directional DC-DC driver for electric vehicles', *2019 1st Global Power, Energy and Communication Conference (GPECOM)*, Nevsehir, Turkey, pp.227–232.

Omotoso, H.O., Alghuwainem, S.M. and Ahmad, I. (2019) 'Constant current fuzzy logic controller for grid connected electric vehicle charging', *2019 8th International Conference on Modeling Simulation and Applied Optimization (ICMSAO)*, Manama, Bahrain, pp.1–5.

Ontiveros-Robles, E., Melin, P. and Castillo, O. (2018) 'Comparative analysis of noise robustness of type 2 fuzzy logic controllers', *Kybernetika*, Vol. 54, No. 1, pp.175–201.

Ravindranath Tagore, Y., Anuradha, K., Vijay Babu, A.R. and Manoj Kumar, P. (2019) 'Modelling, simulation and control of a fuel cell powered laptop computer voltage regulator module', *Int. J. Hydrogen Energy*, Vol. 44, No. 21, pp.11012–19.

Sanchez, M.A., Castillo, O. and Castro, J.R. (2015) 'Information granule formation via the concept of uncertainty-based information with Interval Type-2 Fuzzy Sets representation and Takagi–Sugeno–Kang consequents optimized with Cuckoo search', *Applied Soft Computing*, Vol. 27, pp.602–609.

Wu, G., Ruan, X. and Zhihong, Y. (2015) 'Non-isolated high step-up DC-DC converters adopting switched-capacitor cell', *IEEE Trans. Ind. Electron.*, Vol. 62, No. 1, pp.383–393.

Yadlapalli, R.T. and Kotapati, A. (2014) 'A fast-response sliding-mode controller for quadratic buck converter', *Int. J. of Power Electronics*, Vol. 6, No. 2, pp.103–130.

Yadlapalli, R.T. and Kotapati, A. (2020) 'Implementation of fuzzy logic controller-based quadratic buck converter for LED lamp driver applications', *Int. J. Innovative Computing and Applications*, Vol. 11, Nos. 2/3, pp.159–166.

Yadlapalli, R.T., Narasipuram, R.P. and Dodda, A. (2019) 'Development of fuzzy logic controller for improved interline unified power quality conditioner', *Int. J. Innovative Computing and Applications*, Vol. 10, No. 2, pp.86–99.

Zhang, Y., Fu, C., Sumner, M. and Wang, P. (2018a) 'A wide input-voltage range quasi-Z source boost DC-DC converter with high voltage-gain for fuel cell vehicles', *IEEE Trans. Ind. Electron.*, Vol. 65, No. 6, pp.5201–5212.

Zhang, Y., Zhou, L.M., Sumner, M. and Wang, P. (2018b) 'Single-switch, wide voltage-gain range, boost DC–DC converter for fuel cell vehicles', *IEEE Trans. Vehicular Technol.*, Vol. 67, No. 1, pp.134–145.

Zogogianni, C.G., Tatakis, E.C. and Vekic, M.S. (2019) 'Non-isolated reduced redundant power processing DC/DC converters: a systematic study of topologies with wide voltage-ratio for high power applications', *IEEE Trans. Power Electron.*, Vol. 34, No. 9, pp.8491–8502.